Linear Simulation of the Stationary Eddies in a General Circulation Model. Part I: The No-Mountain Model

SUMANT NIGAM

Department of Earth, Atmospheric, and Planetary Sciences, Massachusetts Institute of Technology, Cambridge, MA 02139

ISAAC M. HELD AND STEVEN W. LYONS[1]

Geophysical Fluid Dynamics Laboratory/NOAA, Princeton, NJ 08542

(Manuscript received 7 March 1986, in final form 18 June 1986)

ABSTRACT

The quantitative validity of linear stationary wave theory is examined by comparing the results from a linear primitive equation model on the sphere with the stationary eddies produced by a general circulation model (GCM). The GCM simulated has a flat lower boundary, so that the stationary eddies can be thought of as forced by heating (sensible, latent and radiative) and time-averaged transient eddy flux convergences. Orographic forcing is examined in the second part of this study. The distribution of the diabatic heating and transient eddy flux convergences and the zonally symmetric basic state are taken directly from the GCM's climatology for Northern winter (DJF). Strong Rayleigh friction is included in the linear model wherever the zonal mean wind is small, as well as near the surface.

The linear model is found to simulate the stationary eddy pattern of the GCM with considerable skill in both midlatitudes and the tropics. Some deficiencies include the inaccurate simulation of the upper tropospheric geopotential over North America and distortion of the wind field near the low-level zero-wind line in the subtropics. Decomposition of the linear solution shows that 1) the extratropical upper tropospheric eddy pattern generated by tropical forcing is significant but smaller than that due to extratropical forcing, 2) the upper-level extratropical pattern deteriorates somewhat when forcing by transients is removed, while the low-level pattern deteriorates dramatically and 3) there is considerable compensation between the effects of low-level thermal transients and extratropical sensible heating, to the point that we argue that this decomposition is not physically meaningful. The sensitivity of the results to the Rayleigh friction formulation is discussed, as is the effect of replacing the transients with thermal damping.

1. Introduction

Linear stationary wave theory continues to provide insights into the time-mean flow in the atmosphere. In such a theory, one takes the zonally averaged flow as given and models the deviations from zonal symmetry in terms of linear forced waves. The pioneering investigation of Charney and Eliassen (1949) showed orography to be a viable forcing mechanism for these waves. A large number of investigators have followed with detailed studies of orographic forcing and the various other mechanisms that are also thought to be important. The role of *extratropical* heating was first modeled by Smagorinsky (1953). The importance of *tropical* heating for asymmetries of the midlatitude flow has become evident from observational studies of interannual variability, notably Bjerknes (1966, 1969) and, more recently, Horel and Wallace (1981), as well as GCM studies of the atmospheric response to SST anomalies, beginning with Rowntree (1972). However, it was not until the work of Hoskins and Karoly (1981) that the relative importance of tropical and extratropical heating was squarely addressed in linear stationary wave models. Strongly contrasting views as to the importance of the tropical component can be found in Simmons (1982) and Jacqmin and Lindzen (1985). The former study suggests that the tropically forced component is a major part of the total stationary wave pattern; the latter suggests that it is only of secondary importance. Zonally asymmetric transient eddy fluxes have also been recognized as important, and are often thought of as damping stationary eddy amplitudes (e.g., Vallis and Roads, 1984). Two noteworthy calculations of the effects of observed transient eddy fluxes in linear stationary wave models are those of Youngblut and Sasamori (1980) and Opsteegh and Vernekar (1982); although their methodologies and conclusions differ in many details, both conclude that the transients are indeed important.

Modern observational studies, including the systematic description of the observed time mean asymmetries (Lau, 1979; Wallace, 1983), have provided modelers with the challenge of simulating not only the

[1] Present affiliation: Geophysics Division, Pacific Missile Test Center, Point Magu, California.

gross features but also details of the observed stationary eddies. Consequently, linear models have become quite sophisticated; multilevel global primitive equation models (with various resolutions in the horizontal and vertical) are now a standard tool for such studies (Hoskins and Karoly, 1981; Simmons, 1982; Hendon and Hartmann, 1982; Lin, 1982; Lindzen et al., 1982; Jacqmin and Lindzen, 1985). We should now be in a position to answer the fundamental question concerning the applicability of these linear models: to what extent do they qualitatively, or even quantitatively, simulate the atmosphere's climatological zonal asymmetries? If the result is sufficiently encouraging, one can go on and examine the relative importance of forcing by different topographic features, extratropical and tropical heating, and transient eddy fluxes.

One of the problems that complicates this task is the lack of a detailed description of the three-dimensional diabatic heating field in the atmosphere. The various published diagnoses, besides being at variance with each other, have mostly been confined to the Northern Hemisphere (some exceptions are the global diagnosis of Schubert and Herman, 1981, the heating parameterization based on observed precipitation rates in Jacqmin and Lindzen, 1985, and FGGE analyses such as that of Wei et al., 1983). In light of this incompleteness and uncertainty, it is difficult to compare solutions to a linear model with observed stationary eddies and conclude that differences are due to neglected nonlinearities. It is also difficult to compare the various stationary wave calculations in the literature, as different workers invariably use different estimates of the diabatic heating field.

The purpose of this two-part study is to determine the qualitative and quantitative validity of linear stationary wave theory by comparing solutions of a steady linear primitive equation model on the sphere with stationary eddies produced by a GCM. The zonally averaged flow about which the model is linearized is taken directly from the time-averaged circulation produced by the GCM. The heating field used to force the linear model is likewise taken to be the time-averaged heating in the GCM. We believe that such a comparison provides a clean test of the linear theory. The GCM need not predict exactly the correct diabatic heating field for this test to be convincing. If the linear model simulates the GCM well, one should expect (in the absence of a dynamical argument that suggests otherwise) the same model to simulate the Earth's atmosphere about as well if given the correct forcing functions. Furthermore, if the linear model simulates the GCM well, it becomes an invaluable tool for diagnosing problems that may be present in the GCM's stationary eddy simulation.

We use the GFDL climate dynamics spectral GCM, with rhomboidal truncation at wavenumber 15. The low resolution has the advantage of permitting extended integrations that allow one to define the time-mean circulation with some precision. This GCM has been integrated both with and without mountains for a period of over 15 years, and the circulation statistics from these integrations have been analyzed by Manabe and Hahn (1981), Lau (1981), Hayashi and Golder (1983a and b), and Held (1983). In Part I of this study we use statistics generated by the GCM in which orography is everywhere set equal to zero; in Part II we use statistics from the standard GCM with realistic orography. In both models, the oceanic surface temperatures are prescribed at their climatological seasonally varying values. Clouds are also prescribed and set to be independent of longitude, a procedure that clearly minimizes the impact of radiative forcing on stationary waves.

There are several reasons why it is useful to begin by simulating a GCM *without* orographic forcing. Orographically forced waves are known to be large, and one therefore expects eddies forced by both heating and orography to be more nonlinear than those forced by heating alone. Also, it is easier to assess the distortion of the thermally forced solution due to the arbitrary (but necessary) inclusion of dissipation near critical surfaces (where the mean zonal wind vanishes) if the large orographically forced wave trains propagating into the tropics are eliminated.

One of the central issues we hope to address is the relative importance of tropical and extratropical thermal forcing for the midlatitude wave pattern. Since one cannot hope to accurately model the extratropical response to a tropical heat source without correctly modeling the tropical response, we emphasize the quality of the tropical flow simulated by the linear model by showing the velocity fields generated by the linear model and not simply the geopotential.

Different authors add a variety of mechanical and thermal damping terms to their models. Rayleigh friction is typically added in the tropospheric interior to remove the critical latitude singularity. The amount of friction needed to remove the singularity depends on the model resolution. However, if we add only enough damping to remove the singularity, the result is a poor tropical simulation when tropical thermal forcing is included. We find that large dissipation is required for the linear model to be quantitatively useful in the tropics. The GCM we are mimicking contains no explicit momentum transport by cumulus convection, so this dissipation is not meant to model "cumulus friction"; rather it models the neglected nonlinearity. If we do not include this large tropical friction, the extratropical solution deteriorates as well. Thus, the difference between our linear model and the GCM is not necessarily a good measure of the total nonlinearity of the wave field. We compromise and try to mimic some of the nonlinearity in a crude way.

The thermal damping added to linear models is often thought of as accounting very roughly for the out-of-phase relationship between the low-level transient eddy

heat flux convergence and the stationary temperature wave, and, to a lesser extent, for the effects of radiation (e.g., Hoskins and Karoly, 1981). We take a different approach by setting the thermal damping to zero and computing the response to transient eddy heat and momentum flux convergences explicitly, (as do Youngblut and Sasamori, 1980, for example). Just as for the diabatic heating field, we take these flux convergences directly from the GCM. We believe that an internal consistency between the diabatic heating field and the eddy flux convergences is essential in such a study. In fact, we believe that it is rather artificial to separate the two, as there is cancellation between small-scale structures in the mean diabatic heating and the mean flux convergences at low levels in the extratropics, and because much of the diabatic heating structure (such as the latent heating in the storm tracks) is itself determined by the transients. However, it seems physically reasonable to try to separate the effects of extratropical *upper* tropospheric transients from the effects of *lower* tropospheric transients *plus* diabatic heating, and this is an aspect of the decomposition we shall emphasize.

We concentrate exclusively in this paper on the stationary eddies in winter (DJF). Following a brief description of the linear model in section 2, we compare the GCM's stationary eddies with the linear response to global heating plus transient eddy flux convergences in section 3. In section 4 we decompose this response into the response to total tropical forcing (heating plus transients) and total extratropical forcing. We also discuss the sensitivity of the response to our frictional parameterization. In section 5 we further split the response to extratropical forcing into parts forced by upper tropospheric transients, lower tropospheric transients, latent, sensible and radiative heating. In section 6 we show how the replacement of the transients by thermal damping affects the solution. Orographic forcing is discussed in Part II.

2. Model description and inputs

a. Description

The linear primitive equation model used in this study is described in detail in a forthcoming paper by Nigam (1987). The primitive equations in σ-coordinates ($\sigma = p/p_s$) are linearized about a zonally symmetric climatology that can include a mean meridional circulation. The linearized equations are shown in section 2 of Nigam (1987), which also contains a description of the meridional and vertical finite-differencing schemes used to find the solution numerically. We have chosen a σ-coordinate model to avoid the need for interpolation when utilizing the GCM's basic state and forcing functions.

The model is "semi-spectral," with the fields Fourier analyzed in the zonal direction but finite-differenced in the meridional and vertical. This configuration was chosen as a compromise between the GCM's structure, which is fully spectral in the horizontal, and the requirements of computational convenience. (With meridional finite-differencing, the matrices that one needs to invert are block-diagonal, or nearly so; with a fully spectral model they are not.) The model uses 101 equally spaced points between the two poles. The zonal dependence of the eddy fields and the forcing are represented by the first 15 zonal wavenumbers (the same resolution as in the GCM). The discretization in the vertical uses nine unevenly spaced σ-levels which are identical to those used in the GCM (0.025, 0.095, 0.205, 0.350, 0.515, 0.680, 0.830, 0.940, 0.990). While the lack of resolution in the stratosphere and mesosphere and reflection from the model top may have some effect on the largest horizontal scales in the GCM's tropospheric stationary wave field, the linear model will have essentially the same bias.

If advection of the zonally asymmetric flow by the mean meridional and vertical velocities is included, the model equations can no longer be reduced to one equation in one variable as in other steady linear primitive equation models. Consequently, the difference equations for zonal velocity, meridional velocity, and temperature at the nine σ-levels and also surface pressure are solved simultaneously using a block matrix formulation. In the present paper, we do not utilize the full generality of the model, and set the mean meridional and vertical velocities in the basic state to zero. The effects of the inclusion of these terms are described in Nigam (1987).

The dissipative terms included in the present model are 1) a linear Rayleigh friction in the horizontal momentum equations, and 2) a small linear ∇^2 diffusion in both the temperature and horizontal momentum equations. The diffusivity is given a constant value (2×10^5 m^2 s^{-1}), and is included for the purpose of smoothing out any small-scale noise in the solutions. It leaves the larger scales virtually unaffected in most cases. Exceptional cases in which the diffusivity has a more significant effect will be noted explicitly. The Rayleigh friction serves two purposes: it mimics planetary boundary layer drag; and it limits the amplitude of stationary eddy velocities in regions where the mean flow is small, and linear, steady wave theory undoubtedly breaks down. The Rayleigh friction coefficient ϵ varies both in the vertical and in the latitudinal direction; it is set equal to the maximum of ϵ_b and ϵ_c, where

$$\epsilon_b^{-1} = 0.2/(\sigma - 0.8), \quad 0.8 < \sigma < 1.0,$$
$$= 0, \quad \sigma < 0.8; \tag{1a}$$

$$\epsilon_c^{-1} = 1.5 \exp[(\Omega/6)^2]. \tag{1b}$$

where $\Omega = \bar{u}/\cos(\theta)$, θ is latitude, $\bar{u}$ is the zonal mean zonal wind in m s^{-1}, and ϵ^{-1} is measured in days.

The ϵ_b represents the frictional retardation of flow near the surface; it decreases linearly from a value of

$(1\ \text{day})^{-1}$ at the surface to zero at $\sigma = 0.8$. It is identical in form to that used by Simmons (1982), but twice as strong. We have not attempted to mimic the GCM's nonlinear stress formulation closely. An average value of the damping of $(2\ \text{days})^{-1}$ within this boundary layer is consistent with the value used by Neelin (personal communication, 1985) in a detailed simulation of the low-level flow in the tropics of this GCM using linear models. Since the boundary layer depth is about a quarter of the scale height, the *e*-folding time for decay of the amplitude of a barotropic eddy is $\approx 4 \times 2 = 8$ days (the *e*-folding time for the energy would be 4 days).

The ϵ_c parameterizes dissipative or "saturation" processes in the vicinity of critical surfaces and is dependent on the strength of the mean zonal angular velocity. It reaches a maximum of $(1.5\ \text{days})^{-1}$ where $\bar{u} = 0$ and quickly falls to negligible values as $|\bar{u}/\cos(\theta)|$ increases beyond 6 m s^{-1}. This functional dependence is clearly arbitrary; it was simply chosen so as to yield a reasonable solution in the tropics, as discussed in section 3, while leaving midlatitudes essentially inviscid. The winter-averaged $\bar{u}$ field of the "no-mountain" GCM is shown in Fig. 1a, and the resulting ϵ^{-1} field in Fig. 1b. Much of the tropical troposphere, including the latitude band (0°–15°S) containing the bulk of the tropical diabatic heat source in northern winter, is damped with a Rayleigh friction coefficient larger than $(3\ \text{days})^{-1}$. Large damping is also present in polar latitudes due to the transition to mean polar easterlies. In the tropics the nonlinearity in the thermodynamic equation is very weak compared to that in the momentum equations, and this is one justification for including the Rayleigh friction in the momentum equations only. While this justification is not relevant for the polar critical surface, we find that our solutions are, in fact, quite insensitive to the dissipation in very high latitudes. More importantly, we shall see that this scheme does not handle the transition from mean westerlies to easterlies in the subtropical lower troposphere very well.

While we do not include thermal damping in most of our calculations, we consider the possibility of replacing the effects of lower tropospheric thermal transients by thermal damping in section 6.

b. *Inputs*

The zonal mean wind, temperature and surface pressure fields about which the model is linearized are obtained by averaging over 15 winters from an extended integration of the "no-mountain" GCM. The zonal wind (Fig. 1a) is similar in its basic structure to the observed wintertime zonal-mean zonal flow. The most significant differences from the point of view of stationary wave theory are most likely the absence of mean easterlies in the tropical upper troposphere and the absence of a clear separation between the wintertime subtropical jet and the middle atmospheric jet.

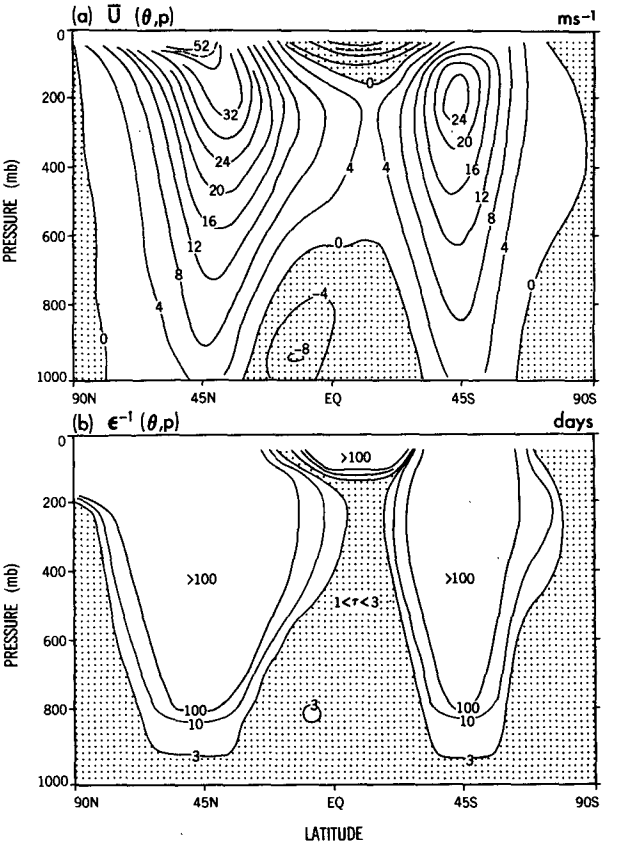

FIG. 1. Latitude–pressure plots of: (a) the wintertime zonally averaged zonal wind from the no-mountain GCM used as the basic state for the linear model, in m s^{-1}, with easterlies shaded; (b) the corresponding reciprocal of the Rayleigh damping coefficient as defined in the text, in days, with values less than 3 days shaded.

Comparison of GCMs with and without mountains shows that the absence of mountains does not appreciably affect either the position or the strength of the zonal mean subtropical jets.

The heating field used as forcing is obtained from the same GCM and consists of radiative heating, sensible heating, latent heating (plus redistribution of heat during convective adjustment), *and* the time-mean convergence of the transient eddy heat fluxes. In order to compute the full transient contribution as accurately as possible, we use the time-mean fields as the initial condition for a one timestep integration of the GCM. The resulting temperature tendency must, by definition, be equal and opposite to the sum of the mean diabatic heating and total transient contribution to the temperature tendency. The mean diabatic heating is accumulated during the GCM integration, and the transient contribution is computed as a residual. The same procedure is followed in computing the total contribution of transients to the tendencies of the zonal and meridional velocities. The contribution of transients to the surface pressure tendency equation in σ-coordinates is ignored.

The vertical average of the total heating is plotted in Fig. 2a, with the zonal mean removed. This total heating is then split into three parts: radiative plus sensible heating, which is dominated almost entirely by the latter in this model (Fig. 2c); latent heating (Fig. 2b); and transient eddy heat flux convergence (Fig. 2d). The total heating is dominated by the three centers of tropical convection, over Africa, Indonesia and South America, and by the two oceanic storm tracks in middle and high latitudes. The latent heating in the storm tracks occurs on the equatorward margins of the total storm track heating. There is considerable compensation on both large and small scales between the transient eddy contribution and the diabatic heating, particularly the sensible heating at high latitudes. The compensation on smaller scales results in the total field being much smoother than the individual components, e.g., over Greenland and Alaska. On the larger scale, the transients move the storm track heating poleward. The total heating clearly reflects the underlying continental distribution, with wavenumber 3 structure in the tropics and wavenumber 2 structure in northern midlatitudes. The vertically averaged heating (with the zonal mean removed) is almost nowhere larger than 2°K day^{-1}.

The differences in vertical structure of the midlatitude and tropical heating fields are shown in Fig. 3a, b, which are longitude–height cross sections of the diabatic heating field (latent plus sensible plus radiative) at 9°S and 45°N, respectively—once again with the zonal mean removed. For presentation purposes, we have averaged the heating rates over the two lowest model layers. This averaging was not used in the linear model calculations we describe (although additional calculations show that the solution at 900 mb and above is very insensitive to the vertical structure of the heating below 900 mb.) The extratropical cross section cuts through the two storm tracks and illustrates the strength of the low-level heating and the rapidity with which it decays with height. In the tropical section one sees the three maxima in convective activity, with the Indonesian heating broader in scale but peaking at a somewhat lower level than the Amazonian and African heating. There are also low-level maxima in the sensible

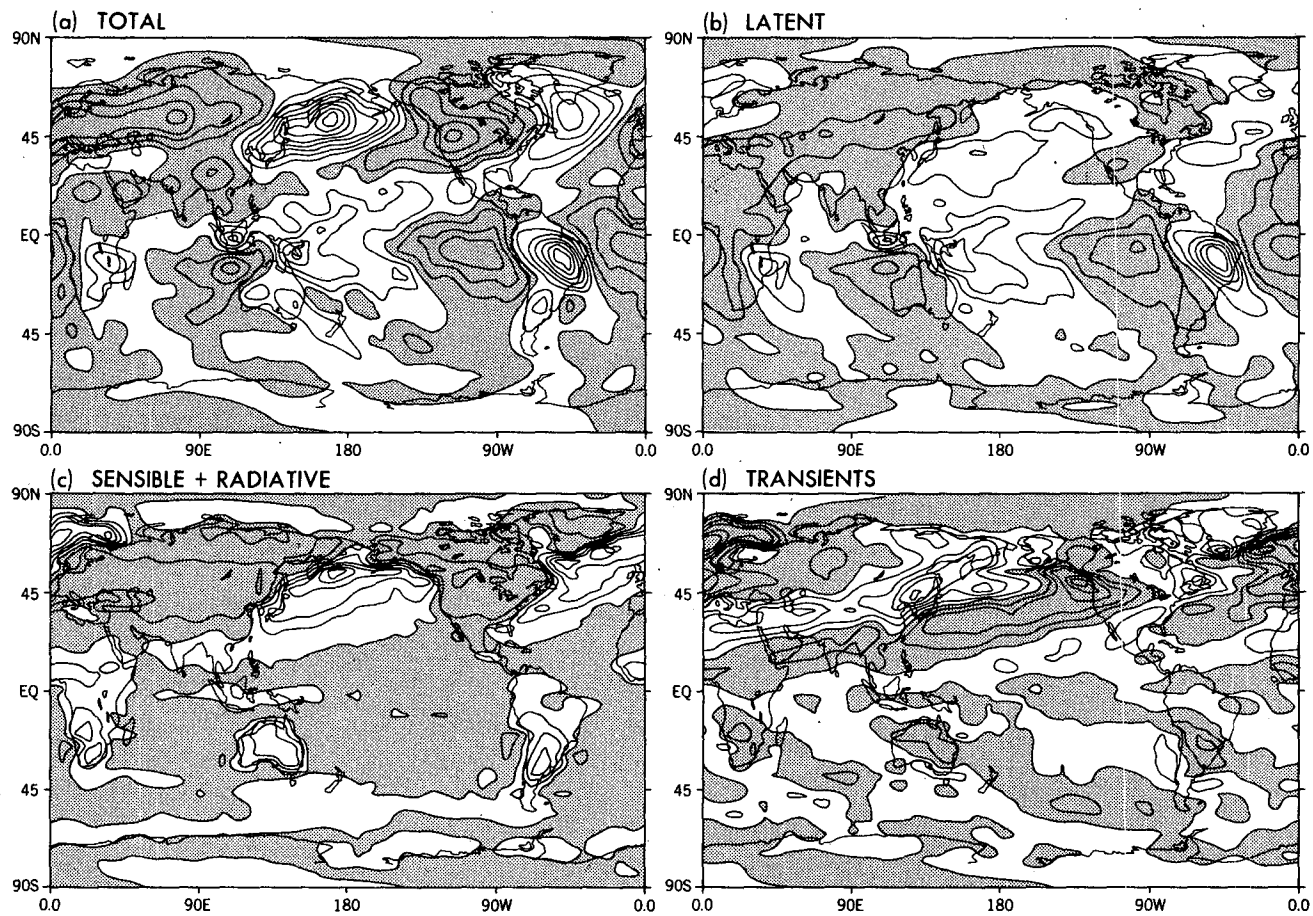

FIG. 2. Vertically averaged heating rates for the GCM's wintertime simulation, with the zonal mean removed, contour interval 0.25°K day^{-1}, and negative values shaded: (a) total heating; (b) latent heat release; (c) sensible plus radiative heating; and (d) heating due to transient eddy fluxes.

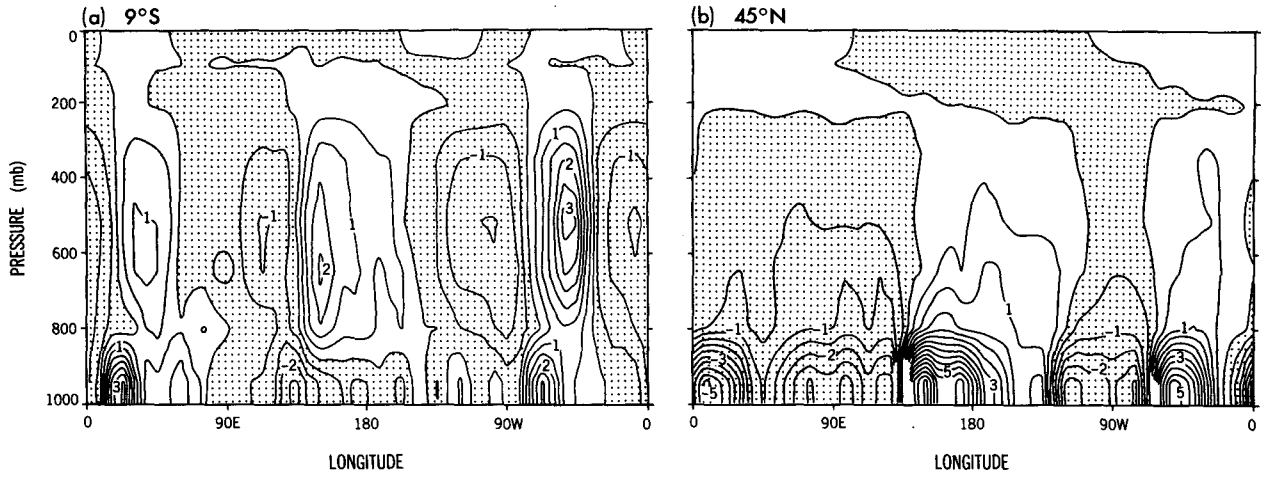

FIG. 3. Longitude–pressure distribution of latent plus sensible plus radiative heating at two selected latitudes. Contour interval is 0.5°K day^{-1}, with negative values shaded.

heating over the African and South American continents, displaced to the west of the midtropospheric latent heating maxima. (The minimum in the sensible heating over Indonesia in this cross section does not correspond to a net cooling, but rather to a heating that is weaker than that at other longitudes.) The structure of the momentum transients will be briefly described in section 5.

3. Comparison of linear model and GCM

The adequacy of linear stationary wave dynamics, and the treatment of the breakdown of linear theory near critical surfaces, is best evaluated by comparing the GCM's stationary eddies with the linear model's response to the total heating field (diabatic heating plus transients) *as well as* the momentum forcing by the transients. The results are shown in Figs. 4 and 5. Figure 4 compares eddy geopotentials at 300 mb and at 900 mb, as well as eddy temperature fields at 700 mb; Fig. 5 compares eddy zonal and meridional winds at 300 mb and zonal winds at 900 mb. Contour intervals for (φ, T, u, v) are (10 gpm, 1°K, 2 m s^{-1}, 1 m s^{-1}), and negative values are shaded. Different variables emphasize different parts of the response. For example, zonal winds emphasize the equatorial flow as well as extratropical Rossby wavetrains with large zonal wavelengths that propagate meridionally; meridional winds highlight extratropical wavetrains with small zonal wavelengths that propagate zonally. Wind fields also tend to be more sensitive indicators of the model's deficiencies than either geopotential or streamfunction. (It is difficult to assess the quantitative validity of the simulated subtropical jet by comparing the streamfunction fields, for example.)

The linear model captures the salient features of the GCM's stationary eddies in both the upper and lower troposphere. A significant discrepancy in the Northern Hemisphere (NH) 300 mb geopotential occurs over northeastern Canada and Greenland, where the linear model generates a trough, while there is only the hint of a trough in the GCM's time mean flow. This discrepancy is fairly robust; in particular, it is not sensitive to the strength of the Rayleigh friction in high latitudes. (Our experience has generally been that the linear model tends to deteriorate at very high latitudes.) The magnitude of the trough off the East Asian coast is underpredicted somewhat, $\approx$90 gpm in the linear model as opposed to 130 gpm in the GCM. On the other hand, the amplitude of the stationary eddies at 300 mb in the extratropical latitudes of the Southern Hemisphere is overpredicted. The structure of the tropical geopotential response at 300 mb is surprisingly good, given the arbitrary dissipation in the linear model.

At 900 mb, the Aleutian and Icelandic lows and the Siberian high are centered at the correct positions and are only slightly too strong. As anticipated, the Siberian high and Aleutian low straddle the shallow heat source in the northwestern Pacific so that the meridional advection of cold air from the north, together with the zonal advection of cold air from the west, balance the heating. However, there is considerable distortion in the subtropics, which we associate with the transition from mean westerlies to easterlies at low levels. This distortion is very evident in the temperature field at 700 mb, although the temperature response north of 40° at this level is excellent. The temperature response tends to deteriorate lower in the atmosphere, most seriously in the subtropics of both hemispheres, so that the simulation of the surface pressure field is less adequate than the simulation of the geopotential at 900 mb.

Turning to the zonal velocities in Fig. 5, one sees that tropical zonal winds in the upper troposphere are of the correct amplitude. In fact, *we have adjusted the strength of the Rayleigh friction to ensure that this be*

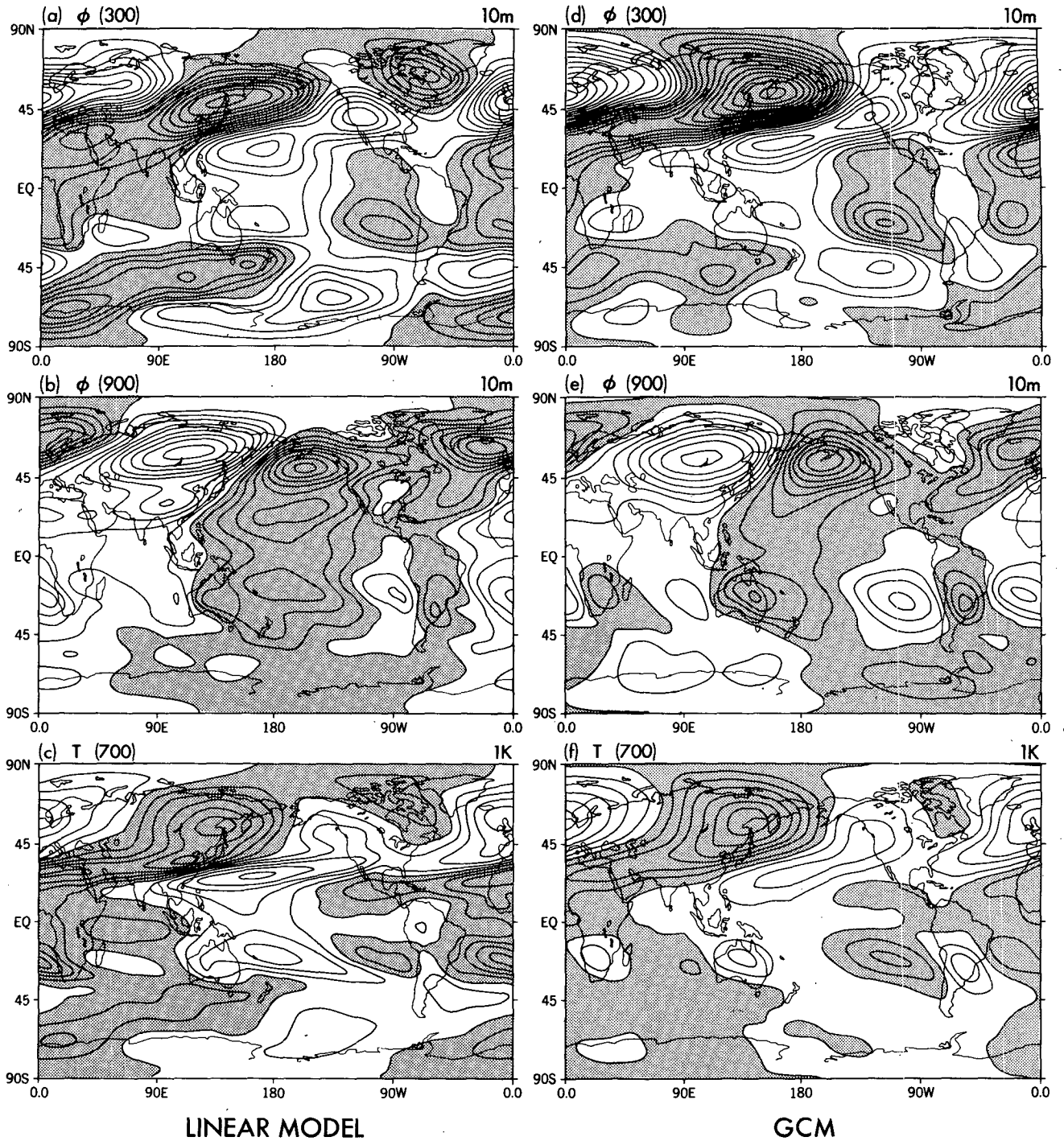

FIG. 4. Stationary eddy fields—(a) geopotential at 300 mb with contour interval 10 gpm; (b) geopotential at 900 mb with contour interval 10 gpm; and (c) temperature at 700 mb with contour interval 1°K—as simulated with linear model, compared with the corresponding fields (d–f) from the GCM's simulation of Northern winter. Negative values are shaded.

the case. The structure as well as the strength of the Walker circulation are captured rather well. The subtropical jet off Japan is located properly but its strength is underpredicted slightly (by ≈15%); however, the strength of the jet off the coast of Australia is overpredicted. The meridional velocity simulation at 300 mb is remarkably good; on the scales that dominate this field, even the solution over North America is fairly

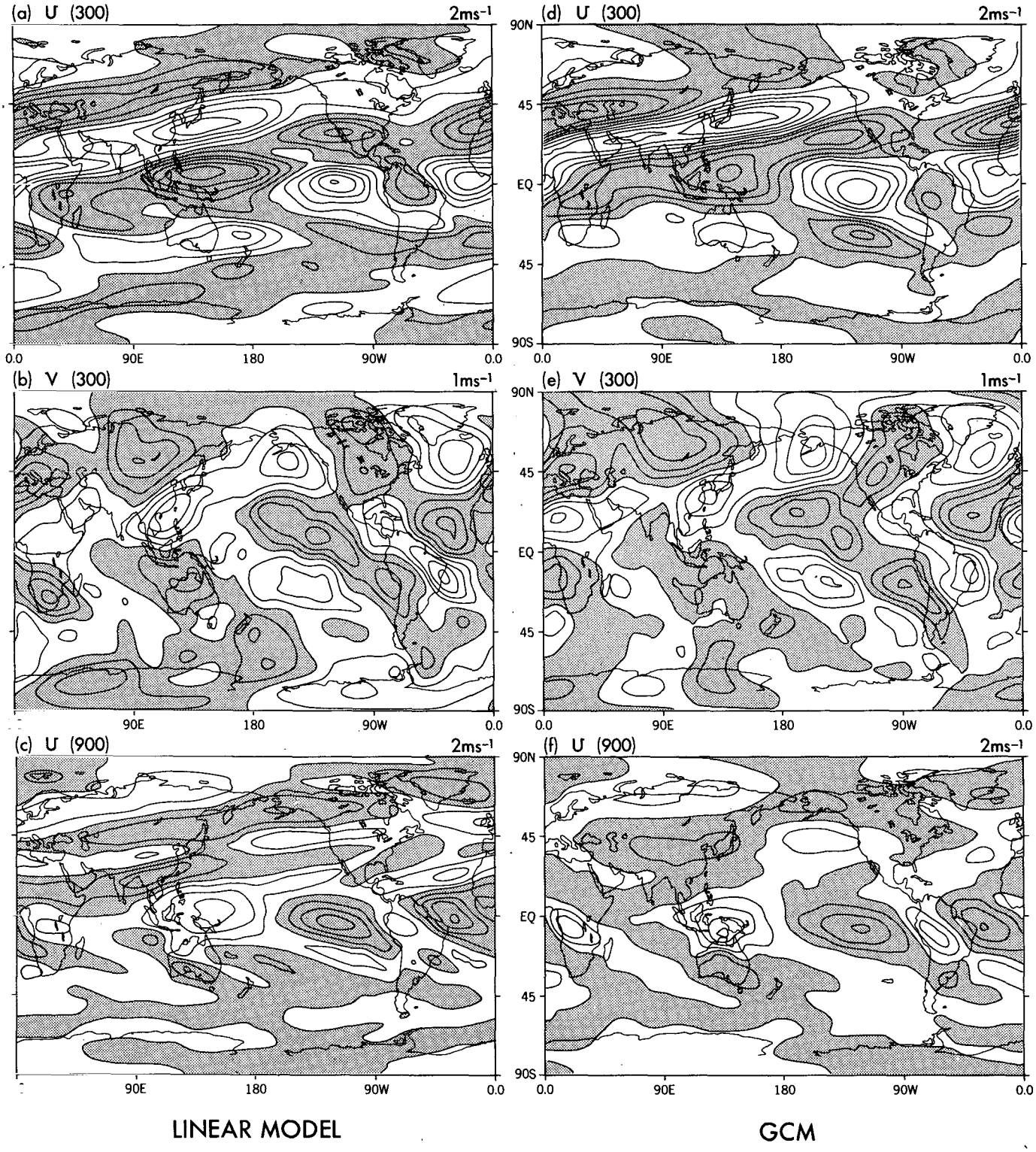

FIG. 5. As in Fig. 4 but for (a) zonal velocity at 300 mb with contour interval 2 m s^{-1}; (b) meridional velocity at 300 mb with contour interval 1 m s^{-1}; and (c) zonal velocity at 900 mb with contour interval 2 m s^{-1}.

accurate. In contrast, the zonal wind at 900 mb shows more clearly than any other the difficulty encountered in the subtropical lower troposphere. An increased thermal diffusion or damping produces more satisfactory low-level subtropical temperature and zonal wind fields, as discussed in section 6. The low-level tropical winds are well simulated [although it should be pointed out that an equatorial beta-plane model linearized about a state of rest can do about as well in simulating the low-level tropical flow (D. Neelin, personal communication, 1985)].

In summary, the solution to the linear model appears to be sufficiently accurate to justify decomposing this response into parts forced by tropical and extratropical heating and by transients in the momentum and temperature equations. The discrepancies may be attributed either to the neglected stationary nonlinearity that is not accounted for by Rayleigh friction, or to the distortion resulting from the frictional parameterization itself, including that of the stress distribution in the planetary boundary layer. Another process that may contribute to differences between the linear model and the GCM, and one that can be included within the framework of the steady linear model, is the advection of eddies by the mean meridional circulation $(\bar{v}, \bar{\omega})$; this is discussed in a forthcoming paper by Nigam (1987).

4. Tropical versus extratropical forcing

We take the total heating field (diabatic forcing plus heating due to transients) plus the momentum forcing by transient eddies, and divide it into two parts. The "extratropical" part is obtained by setting the forcing to zero south of 15°N; the remainder is referred to as the "tropical" part. The choice of 15°N is based on an inspection of Fig. 2, which shows there to be a sharp distinction in the Northern Hemisphere between heating associated with the storm tracks north of 30°, and the tropical convective heating located primarily south of the equator. There is little eddy heating in the vicinity of our 15°N boundary. The distinction between convective and "storm track" heating is less clear in the summer hemisphere, and we have simply lumped all of the Southern Hemisphere sources into the "tropical" component.

We find in the lower troposphere that the extratropical part of the response is almost entirely forced by extratropical sources and the tropical part by tropical sources, so we do not bother to display these results. The extratropical geopotential response at 900 mb to the tropical forcing is at most 20 gpm. The situation in the upper troposphere is more complex.

The 300 mb zonal wind and geopotential responses to the tropical and extratropical forcing components are shown in Fig. 6. It is clear that the upper tropospheric tropical eddies are primarily forced by the tropical sources. However, the extratropically forced perturbations to the zonal wind penetrate to ~10°N with amplitudes of 5 m s^{-1}, and at these latitudes they do modulate the tropical response appreciably. In particular, the positive u' perturbation over East Africa and Southeast Asia does improve the agreement with the GCM. Despite the weak upper tropospheric westerlies in the basic state, the effect of the Northern Hemisphere extratropical source on the Southern Hemisphere eddies is negligible in our model.

The extratropically and tropically forced components are both significant northward of 20°N, with the former being dominant. The extratropically forced wave field in the upper troposphere is dominated by zonal wavenumber 1; the meridional scale must then be small for the total horizontal wavenumber to be comparable to the Rossby stationary wavelength, and this is observed in the solution. The SW–NE phase tilt south of 50°N is a clear indicator of southward propagation, the heating contrast between Siberia and the western North Pacific being the dominant source. The extratropical forcing alone places the largest subtropical jet maximum over the central Pacific at ≈40°N, with strength 6 m s^{-1} greater than the zonal mean. The corresponding low in the North Pacific reaches 70 gpm.

The tropically forced component in midlatitudes has the now classic structure of arcing Rossby wave trains. There is a remarkable degree of symmetry between the two hemispheres, with the amplitude of the geopotential response rising to slightly more than 40 gpm. Since the amplitude of the stationary waves in the Southern Hemisphere is overestimated somewhat, it seems unlikely that the Northern Hemisphere response is being underestimated. The tropical response creates a subtropical jet maximum of 5 m s^{-1} south of Japan. The combination of the tropically and extratropically induced jets create a pattern in reasonable agreement with the GCM, but slightly weaker in amplitude. The superposition of the geopotential structures is complex, with regions of constructive interference (e.g., off the coast of Asia) and destructive interference (e.g., over Alaska). It seems that the error in the linear simulation over eastern North America is more likely due to extratropical than to tropical forcing.

In Fig. 7 the tropically forced response is split into parts forced by sources in the eastern and western hemispheres (more precisely, the boundaries are taken to be 0° and 150°W). The eastern hemisphere source is dominated by the Indonesian heating, and the western by the Amazonian heating. The Northern Hemisphere geopotential response at 300 mb is shown in stereographic projection. We find that the wave train over the Pacific is entirely forced by the eastern hemispheric heating, while the Amazonian heating is responsible for a wavetrain propagating north and then east across the North Atlantic and Europe. As the Indonesian response also penetrates into the western hemisphere, the response there is the superposition of a wave train with large zonal scale propagating merid-

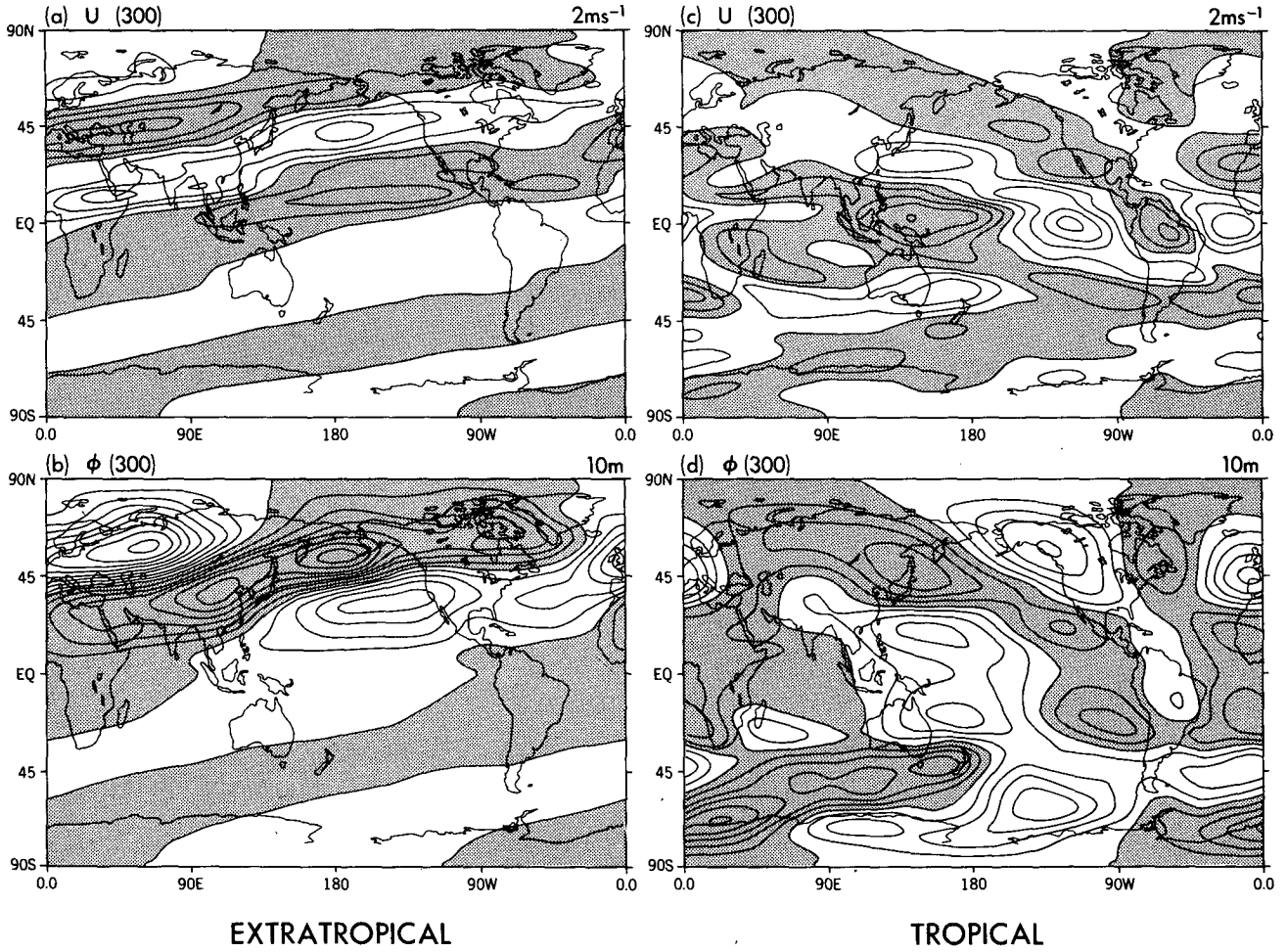

FIG. 6. Decomposition of the 300 mb zonal velocity and geopotential produced by linear model into parts forced by extratropical heating plus transients (a–b) and tropical heating plus transients (c–d). Contour interval and shading as in Figs. 4 and 5. "Extratropical" is defined as north of 15°N; equatorward is "tropical."

ionally and a wave train of smaller zonal scale with a more zonally directed group velocity.

The Indonesian heating, with a maximum vertically averaged strength of slightly greater than 1 K day^{-1}, produces an extratropical response of 30–40 gpm at 300 mb in our linear model; the Amazonian heating, more intense but also more localized, produces an extratropical response of $\approx$20 gpm. In making comparisons with the amplitudes of extratropical wave trains generated in other models, one must keep in mind the sensitivity of such models to the relative position of the heat source and the zero-wind line in the basic zonal flow and the sensitivity to dissipative parameterizations. The importance of the zero-wind line's location is emphasized by Jacqmin and Lindzen (1985), among others. Keeping this sensitivity in mind, we find that Jacqmin and Lindzen's estimate of the tropically forced wave train is comparable in amplitude (and structure) to ours (however, their estimated response to extratropical heating bears little resemblance to ours). Hoskins and Karoly (1981) also obtain $\approx$40 gpm for a 1 K day^{-1} vertically averaged heating rate. Simmons' (1982) response, when scaled down to 1 K day^{-1} forcing and ignoring differences in horizontal structure, yields 80 gpm. Simmons' heating is broad meridionally, and extends well into the region of mean westerlies (and well away from the equator, so that one obtains more vortex stretching for a given vertical velocity); he also uses an ϵ_c that decreases away from the critical surface much more rapidly than ours.

Hendon and Hartmann (1982) also make clear the sensitivity of the extratropical wave train to the dissipation mechanisms present (see their Fig. 12). The sensitivity of our results to the Rayleigh friction is illustrated in Fig. 8. Two cases are depicted. On the left-hand side we show the 300 mb response to the total tropical forcing when the maximum value of ϵ_c in Eq. (1b) is lowered from (1.5 days)$^{-1}$ to (10 days)$^{-1}$. Com-

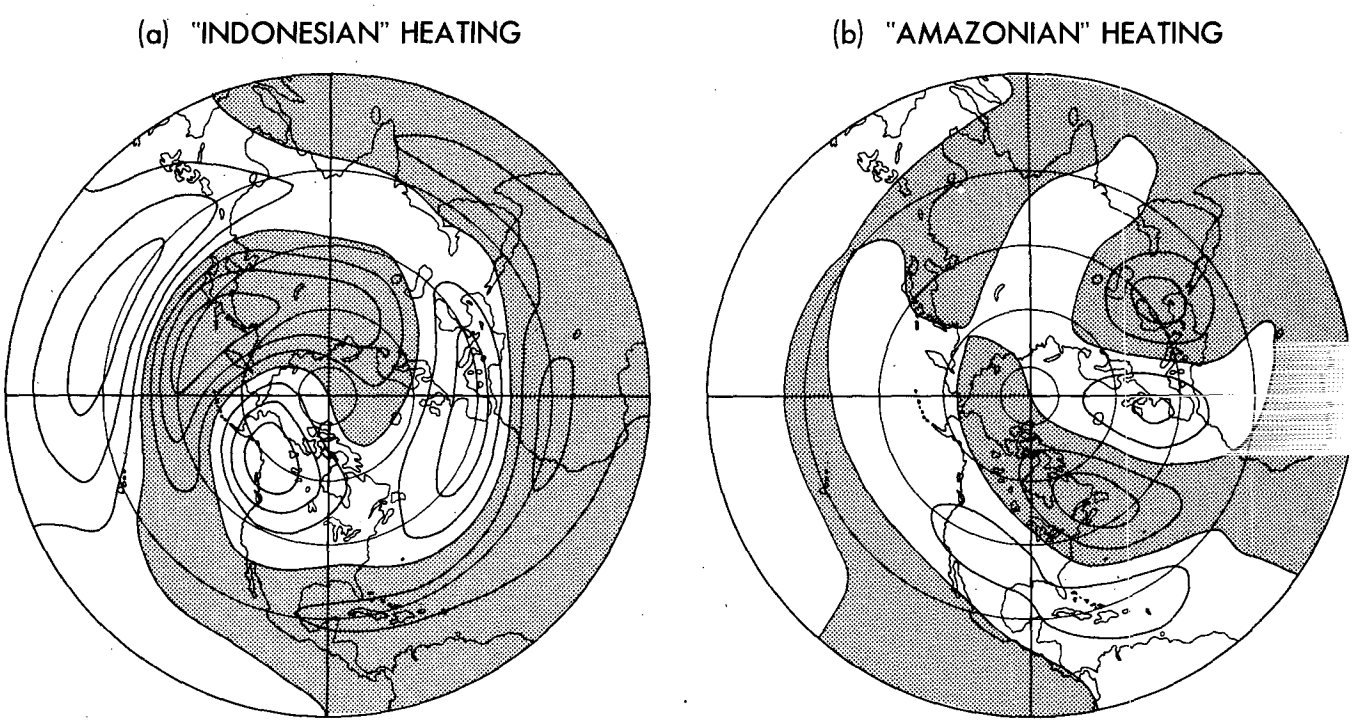

FIG. 7. The tropically forced geopotential at 300 mb split into parts forced in the longitude intervals (a) $0° < \lambda < 150°W$, referred to as the "eastern hemispheric" or "Indonesian" component, and (b) $150°W < \lambda < 0°$, referred to as the "western hemispheric" or "Amazonian" component. The Northern Hemisphere is shown in polar stereographic projection, with a contour interval of 10 gpm and with negative values shaded.

paring with our standard case (the right half of Fig. 6) we see that the tropical zonal winds are now much stronger—more than a factor of 2 in the western hemisphere, less over Indonesia—in clear disagreement with the GCM. Fortunately, the contribution of the tropical forcing to the subtropical jet off Japan is much less sensitive to ϵ_c, although the maximum has moved equatorward and westward with decreased drag. In the geopotential (Fig. 8b), the dominant wave train emanating from the Indonesian heating is attenuated and shifted westward by $\sim 30°$ of longitude in comparison with that in Fig. 6d. We find that this causes the simulation of the total field to deteriorate somewhat as an *eastward* phase shift is needed to improve the simulation. The smaller value of ϵ_c also results in an anomalous wave train of short zonal scale that propagates zonally downstream across Europe (most noticeable over the Mediterranean) and then across South Asia. As is evident from inspection of Figs. 7 and 8, the source is the Amazonian heating. There is no clear sign of this wave train in the GCM stationary wave field. If one examines the v'-field (not shown), rather than the geopotential, the excellent agreement between GCM and linear model seen in Fig. 5 is destroyed quite dramatically. With weaker damping, the response in the subtropics of the Southern Hemisphere is also much stronger, resulting in an even larger disagreement with the GCM in that hemisphere.

On the right-hand side of Fig. 8 we show the response to tropical forcing when our formulation for ϵ_c is replaced with Simmons': $\epsilon_c^{-1} = 2[\bar{u}/\cos(\theta)]^2$ days (with $\bar{u}$ in m s^{-1}). Although the damping strength where $\bar{u} \approx 1$ is comparable to that in our standard case, it drops much more quickly with increasing $\bar{u}$ (with $\bar{u} = 4$ m s^{-1} at the equator, $\epsilon_c^{-1} = 32$ days in Simmons' formulation, and ~ 2.5 days in ours). The result is effectively weaker damping in the region of strongest heating and a flow field that is comparable to our weakly damped case. The anomalous zonally propagating wave train over Europe is even more pronounced. If we remove the small ∇^2 diffusion in the model (see section 2), the anomalous wave train is amplified still further.

The model's sensitivity to the Rayleigh friction is complex. While the sensitivity of the tropical zonal winds could likely be captured qualitatively in a model linearized about a state of rest (even with a shallow water model, e.g., Gill, 1980), some parts of the extratropical wave field are more sensitive to the tropical damping than others. Evidently, the wave field generated by the model's sharp and deep Amazonian heating must be damped strongly to simulate the GCM.

Rayleigh friction coefficients as large as those used in the present study in the deep tropics have rarely been used in linear, multilevel primitive equation models, presumably because little attention has been paid to details of the tropical simulations in these mod-

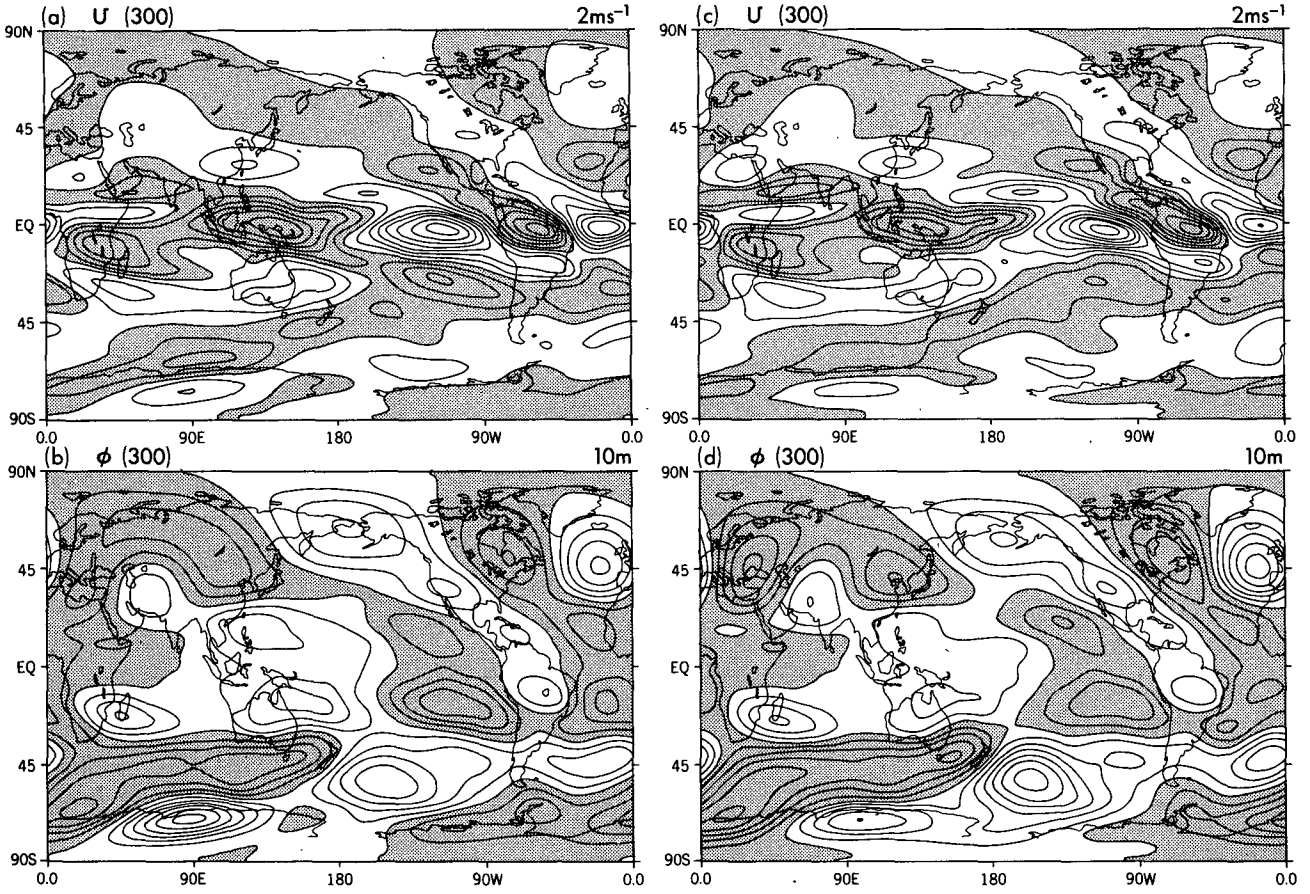

FIG. 8. The tropically forced zonal wind and geopotential at 300 mb as predicted by the linear model with modified Rayleigh friction in the free atmosphere ($\sigma < 0.8$): (a) and (b) with $\epsilon_c^{-1} = 10 \exp[(\Omega/6)^2]$; (c) and (d) with $\epsilon_c^{-1} = 2\Omega^2$ as in Simmons (1982). Contours and shading as in previous figures. For notation, refer to Eq. (1) in text.

els. However, large damping has become customary in barotropic or shallow-water models of the steady tropical upper tropospheric circulation (Holton and Colton, 1972; Chang, 1977; Gill, 1980), where it has often been justified as parameterizing the vertical mixing of momentum by deep cumulus convection. The GCM we are simulating has no subgrid-scale vertical mixing of momentum above the boundary layer, so our large damping most likely represents nonlinear saturation effects of the sort discussed by Sardeshmukh and Held (1984) and Sardeshmukh and Hoskins (1985). Hopefully, the disturbing sensitivity of linear models to arbitrary damping would be alleviated somewhat in nonlinear models of the steady response to tropical heating. (The tropical lower tropospheric response is also sensitive to damping, but primarily to the surface stress formulation, ϵ_b, and not to the much more arbitrary interior damping, ϵ_c.)

We can further divide the response to "tropical forcing" into the part forced by diabatic heating and the part forced by transient eddy fluxes of heat and momentum. In the Northern Hemisphere extratropics and in the tropical upper troposphere, the total response is similar to the response to diabatic heating alone. (The response to the Amazonian heating is once again more sensitive to the inclusion or omission of the transient forcing; the same is also true for parts of the lower tropospheric response. Most of this effect is unexpectedly due to transients in the thermodynamic equation, presumably due to a correlation in time between the vertical motion and the lapse rate, rather than to transients in the momentum equations.) Our "tropical forcing" contains all of the forcing in the Southern Hemisphere as well, and the part of this forcing explicitly due to transients makes a large contribution to the pattern in the Southern Hemisphere middle and high latitudes. In fact, there is considerable cancellation between the responses to transient forcing and the response to diabatic heating of the sort we describe in detail for the Northern Hemisphere in section 5.

5. The response to extratropical forcing by transients, latent and sensible heating

We now focus on the extratropical Northern Hemisphere and decompose the response further. In partic-

ular, we divide the forcing of the stationary waves by extratropical transient fluxes into upper and lower tropospheric parts, for two distinct reasons. First, as suggested by observational studies (most recently, Randel and Stanford, 1985) and by baroclinic eddy life cycle calculations (Simmons and Hoskins, 1978), one can think of the mixing induced by upper and lower tropospheric extratropical transients in distinctly different ways: the lower tropospheric mixing is generated during the growth stage of baroclinic disturbances; the upper tropospheric mixing is generated during barotropic decay (see Held and Hoskins, 1985, for further discussion). Second, lower tropospheric transient heat fluxes are so intimately related to the diabatic heating field that it is convenient to group them together.

Given the local tendencies $\partial u'/\partial t$ and $\partial v'/\partial t$ due to momentum transients, one can compute a vorticity tendency and, by operating with the inverse Laplacian on the sphere, a streamfunction tendency. Figure 9a shows the streamfunction tendency due to the extratropical momentum transients averaged over the upper troposphere. We use the same definition of "extratropical" as in section 4, and we define the "upper troposphere" as the top five layers in the model, the lower boundary of which is roughly at 600 mb. Only the streamfunction tendency in the Northern Hemisphere is shown in the panels. This streamfunction tendency peaks at 300 mb, where it has roughly the same structure as in Fig. 9a, but with three times the amplitude. Figure 9b is a similar plot for the lower troposphere where, as anticipated, the amplitudes are much smaller. Integrating vertically over the whole atmosphere, the streamfunction tendencies are of the order of 5 $m^2 s^{-2}$ in midlatitudes; at 300 mb they are $\sim 30\ m^2 s^{-2}$.

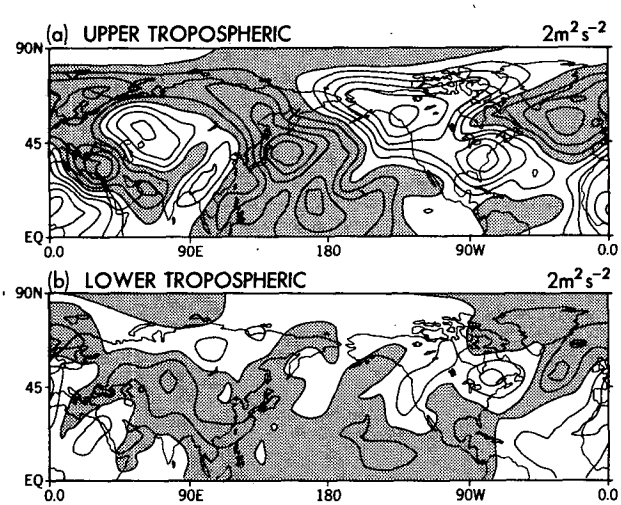

FIG. 9. Streamfunction tendency in the Northern Hemisphere due to extratropical (north of 15°N) transients in the momentum equations of the no-mountain GCM averaged over (a) the upper troposphere (above 600 mb) and (b) the lower troposphere (below 600 mb). Contour interval is 2 $m^2 s^{-2}$, with negative values shaded.

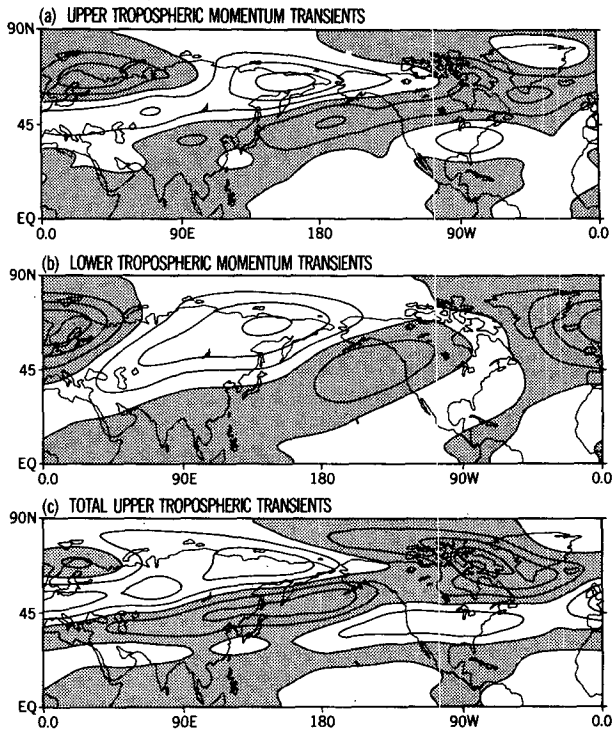

FIG. 10. 300 mb geopotential in the Northern Hemisphere produced by the linear model when forced with (a) upper tropospheric extratropical transients in the momentum equations, (b) lower tropospheric extratropical transients in the momentum equations, and (c) upper tropospheric extratropical transients in the momentum and thermodynamic equations. Contour interval is 10 gpm, with negative values shaded.

The 300 mb response to the upper tropospheric extratropical momentum transients predicted by the linear model is displayed in Fig. 10a. The amplitudes are modest, rising to little more than 30 gpm, and there is little visual resemblance with the streamfunction tendency in Fig. 9a. In Fig. 10b, we plot the response at 300 mb to the lower tropospheric momentum transients. Given the very large disparity between the size of the momentum forcing in the upper and lower troposphere, as indicated in Fig. 9, it is, at first sight, surprising that the linear responses at 300 mb are comparable. The reason is simply that the larger vorticity or streamfunction tendencies at upper levels occur in the presence of much larger zonal winds. The stronger the wind, the less time a parcel of air spends in a region of forcing, and the smaller the response. It is therefore misleading to take the relative importance of upper or lower level transients in tendency calculations of the sort described in Lau and Holopainen (1984), for example, as indicative of their relative importance for the stationary eddy structure. The response at 300 mb to the total momentum forcing, the sum of Fig. 10a, b, amounts to 60 gpm in high latitudes. The response at 900 mb is ~20 gpm. While not insignificant, we

find that the agreement between the linear solution and the GCM is not hurt appreciably if we omit the momentum forcing entirely. In fact, there is a slight improvement (in particular, the prediction over North America improves); we do not understand why.

Figure 10c shows the response to upper tropospheric extratropical momentum *plus* thermal transients, and indicates that thermal transients in the upper troposphere also contribute a modest amount to the upper tropospheric wave pattern. There is little tendency for cancellation between the responses to the upper tropospheric momentum and thermal transients. The response to the low-level momentum transients should similarly be combined with that due to the low-level thermal transients, as both of these are presumably generated during the same wave propagation and mixing events; however, the low-level thermal transients present additional problems, as described here.

Figure 11 shows the 300 mb geopotential responses to a) the sum of the total extratropical diabatic heating and lower tropospheric thermal transients, b) extratropical latent heating only, c) extratropical sensible plus radiative heating, and d) extratropical lower tropospheric thermal transients. The top panel (a) is the sum of the other three and it is broadly similar to the total extratropical response (Fig. 6b), since the response to momentum forcing plus upper level thermal transients (the sum of Fig. 10b, c) is comparatively modest. The amplitude of the response to extratropical latent heating (Fig. 11b) is comparable to that generated in midlatitudes by the tropical latent heating (~40 gpm). Extratropical latent heating alone produces a jet maximum in the eastern Pacific. The contribution of sensible plus radiative heating in Fig. 11c is predominately due to sensible heating (as noted earlier, the GCM has zonally symmetric clouds, which minimizes the zonal asymmetries in the radiative heating). The 300 mb response to low-level thermal transients (Fig. 11d) is somewhat smaller than the sum of the responses to latent and sensible heating, except in very high latitudes. Noting that the total 300 mb response to extratropical forcing (Fig. 6b) is the sum of Figs. 11a, 10b and 10c, it seems that the spurious linear simulation over Hudson Bay and northeastern Canada is at least partly due to the response to upper tropospheric transients.

Equatorward of ~45°, the response forced by extratropical sensible heating is roughly in phase with that forced by extratropical latent heating. However, northward of 60° the response to sensible heating is almost entirely canceled by the response to low-level thermal transients. The cancellation suggests that this decomposition may be physically misleading. The sensible heating and transient flux convergence both have structures of very small scales in high latitudes which cancel (see Fig. 2). The transients can presumably be thought of as smoothing the heating field in a more or less diffusive manner. If we increase the diffusivity in the linear model, or if we include thermal damping, the large response in Fig. 11c north of 60° disappears. We return to this point in section 6.

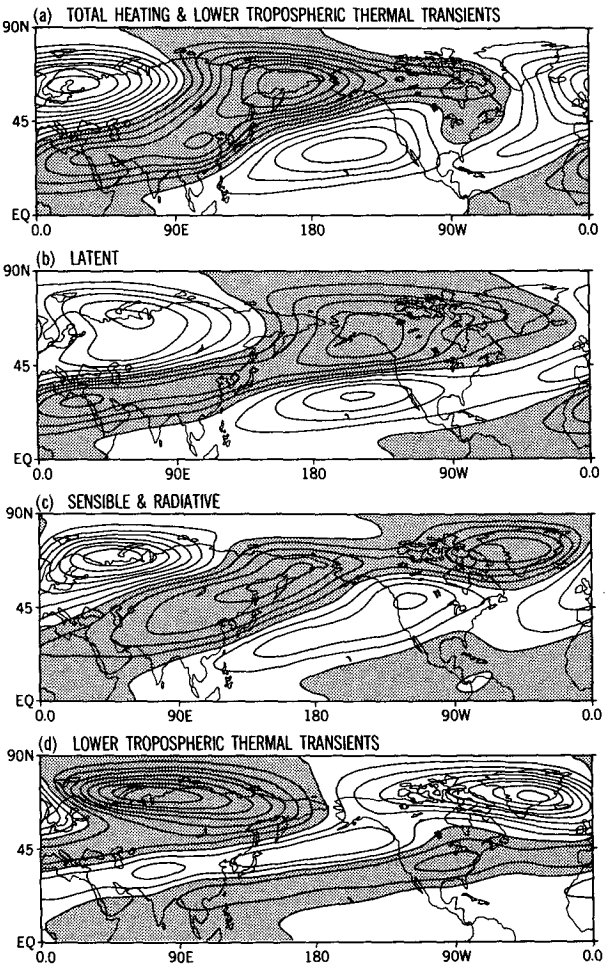

FIG. 11. 300 mb geopotential in the Northern Hemisphere produced by the linear model when forced with (a) total extratropical diabatic heating (latent plus sensible plus radiative) plus lower tropospheric transients in the thermodynamic equation, (b) extratropical latent heating only, (c) extratropical sensible plus radiative heating only, and (d) extratropical lower tropospheric transients in the thermodynamic equation only. Contours as in Fig. 10.

Figure 12 shows the 900 mb responses in a format identical to Fig. 11. The relative importance of the various components is now quite different, with the heating by low-level transients dominant. The total response to extratropical heating plus low-level thermal transients (Fig. 12a) is similar to the response to the total forcing (Fig. 4b), and even more similar to the GCM's geopotential at 900 mb shown in Fig. 4e (the amplitudes and locations of the major highs and lows are somewhat improved). Latent heating (Fig. 12b) produces much of the pattern south of 45°, but cannot explain the positions or amplitudes of the oceanic lows and Siberian high. The sensible heating response (Fig.

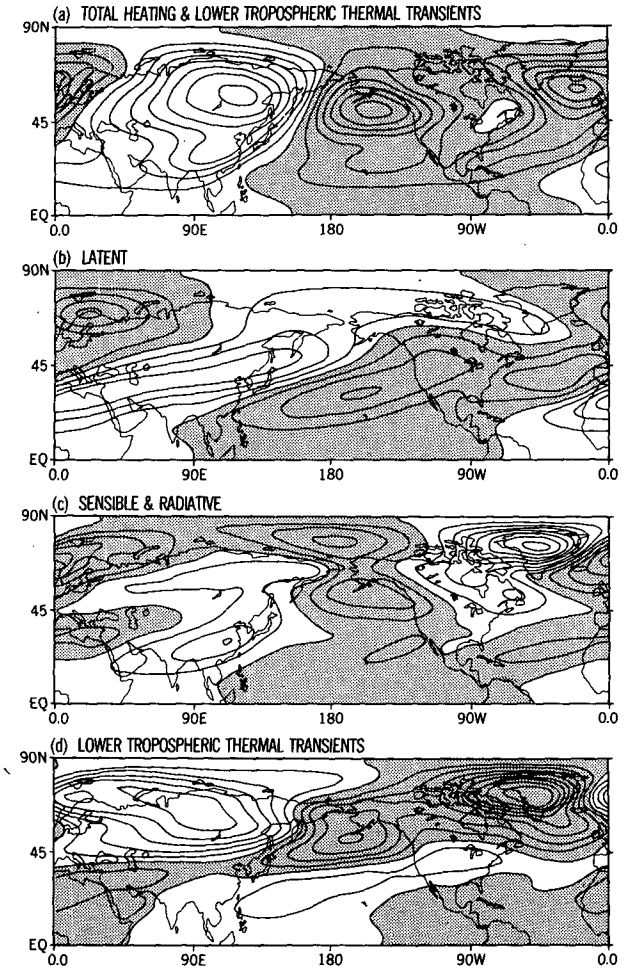

FIG. 12. As in Figure 11 but for the 900 mb geopotential.

12c) is again complicated by large amplitudes in very high latitudes, particularly near Greenland and Scandinavia, that are canceled by the response to transient heating (Fig. 12d). (Reference to the heating rates in Fig. 2 shows the small scale structure responsible for this cancellation.) The high over China in this low-level response, which is in disagreement with the GCM, (see Fig. 4b), is generated by sensible heating, rather than latent heating or transients.

6. The linear response with thermal damping replacing the forcing by transients

Much of what we refer to as "forcing" in these linear calculations is in fact a complex and little understood function of the true boundary conditions and the stationary eddy pattern itself. It is particularly unsatisfying to consider the transient eddy fluxes as external forcing, as is made very clear by the near cancellation between the response to transients (primarily the thermal transients) and the response to sensible heating in high latitudes. If one omits the transient forcing completely, the most serious discrepancies occur near the surface in high latitudes, as described in section 5. The cancellation between the responses to sensible heating and low-level thermal transients then suggests that useful results could be obtained by omitting the transient forcing and including thermal damping or diffusion in its place.

We describe one preliminary attempt along these lines, in which we remove the transient forcing and add a thermal damping to the model, with an e-folding time of 5 days at the surface, rising linearly in pressure to 20 days at 200 mb, and remaining at 20 days above 200 mb. (This is similar to the thermal damping used by Hoskins and Karoly, 1981.) In Fig. 13, we show the resulting 300 mb and 900 mb zonal winds and geopotentials, the 300 mb meridional wind, and the 700 mb temperature. The upper level response is now somewhat weaker than that forced by total heating plus transients (Figs. 4 and 5); the perturbation zonal wind maximum off Japan is now ~ 7 as opposed to ~ 9 m s^{-1}, while the geopotential amplitudes are now no larger than 65 gpm. The amplitude of the temperature perturbations at 700 mb is also reduced by as much as 30%. On the other hand, the temperature structure in the subtropics is smoother, as compared with the model results in Fig. 4c, and the small-scale structure in the zonal wind at low levels near the subtropical transition from easterlies to westerlies is also more reasonable. However, the thermal damping does not capture the effects of the GCM's thermal transients in moving the oceanic lows and Siberian high to higher latitudes, and the resulting 900 mb geopotential in the extratropics resembles the response to latent heating alone, shown in Fig. 12b. Further analysis of the solutions shows that the response to sensible heating (not shown) is now much smaller, rising to no more than 20 gpm, with hardly a trace of the large response at high latitudes in Fig. 12c. As expected, the response to tropical forcing is found to be relatively insensitive to thermal damping because the balance between vertical motion and tropical heating in the thermodynamic equation is robust. Thus, excepting the regions where forcing by thermal transients is important (e.g., over the Amazon and in parts of the tropical boundary layer), the tropical circulation shown in Fig. 13 is similar to that in Fig. 5.

A height-dependent thermal damping is clearly an extremely crude attempt at parameterizing the effects of transients. We show these results to point out that thermal damping of the sort used in other models has a significant effect on our solutions, and that care must be taken in comparing models with different dissipative parameterizations. We have found that replacing the height-dependent thermal damping with a large height-dependent thermal diffusivity produces similar results, with similar deficiencies. Our suspicion is that one could do better with a diffusivity that depends on latitude as well as height. It goes without saying that a

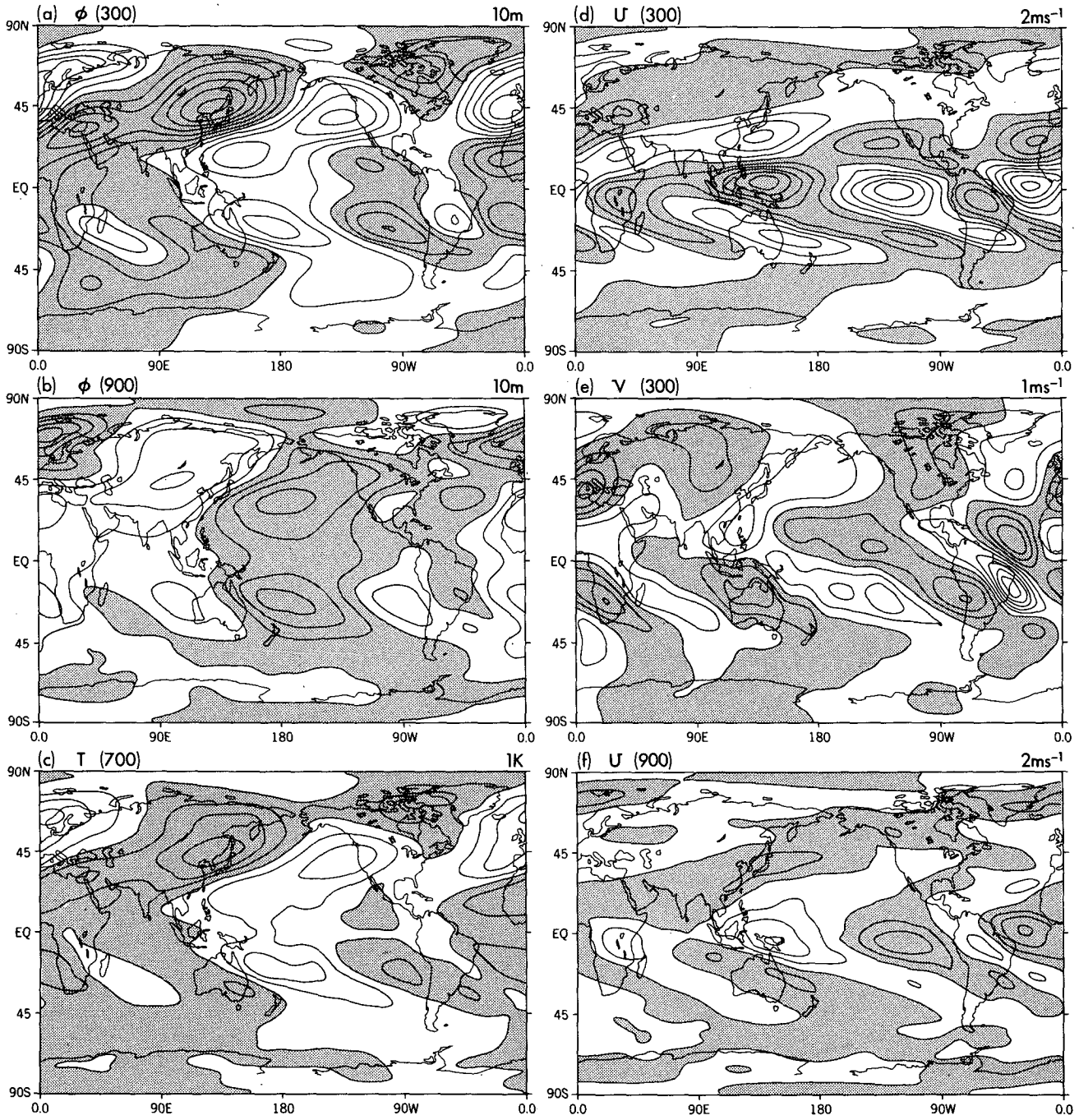

FIG. 13. Stationary eddy fields produced by the linear model when forced by the total diabatic heating (latent plus sensible plus radiative) but *without* forcing by transient eddies, and including thermal damping as described in text. Contour intervals as in Figs. 4 and 5.

parameterization scheme on a sound theoretical footing would be far more satisfying.

7. Conclusions

We find that a linear primitive equation model on the sphere can provide useful simulations of the stationary wave field produced in NH winter by a GCM with a flat lower boundary. The amplitudes are underpredicted slightly (10%–30%) in the NH extratropical upper troposphere and overestimated somewhat in the SH, but nearly all major features of the model's stationary wave field are captured with some fidelity.

Given this linear simulation, we determine how much of the stationary wave field is generated by tropical and how much by extratropical forcing. In the NH

extratropics, the response to tropical forcing is significant in the upper troposphere but the response to the extratropical forcing is larger. The two patterns interfere constructively in some regions and destructively in others. Quantitative conclusions are somewhat suspect due to the arbitrariness of the tropical damping, which controls the strength of the tropical response to tropical heating and also affects the Rossby wave trains ejected into midlatitudes. The response to Amazonian heating is found to be more sensitive to this damping than the response to Indonesian heating, suggesting that the former is more strongly nonlinear in the GCM.

We further divide the response into the part forced by the mean heating and the part forced by transients. The tropical response is little affected by the transient forcing. In the extratropics, the response to upper tropospheric transients ($p < 600$ mb) is small (<30 gpm) in both upper and lower troposphere. There is considerable cancellation between the response to lower tropospheric transients (mostly thermal transients) and the response to sensible heating at high latitudes, a consequence of the smoothing by the low-level thermal transients of sharp small-scale structures in the sensible heating field. Given this cancellation, we do not believe it is very useful to study the stationary wave response to transient eddy fluxes in isolation from the response to sensible heating. The simulation deteriorates dramatically at low levels if transient forcing is simply omitted. If the transient forcing is replaced by thermal damping, the solution is better behaved, as it is then less sensitive to details of the sensible heating in high latitudes; in addition, the solutions are much smoother near the surface at the subtropical transition from mean easterlies to westerlies. However, the amplitude of the extratropical upper tropospheric eddies is reduced, while the low-level oceanic lows and Siberian high are incorrectly placed. These results serve to reemphasize the importance of a parameterization of low-level transients for any theory of the time-mean low-level flow. The response to latent heating alone produces a poor simulation of the low-level extratropical geopotential. The response to radiative heating is negligible in this GCM.

We believe that such linear models are invaluable as tools for analyzing GCMs. They also point out difficulties that must be faced when trying to understand stationary eddies in the atmosphere. The two difficulties highlighted by this study are the tropical nonlinearities and the relationship between the extratropical sensible heating and low-level thermal transients.

Acknowledgments. A preliminary version of this work constitutes part of the Ph.D. dissertation of S. Nigam in the Geophysical Fluid Dynamics Program at Princeton University. We would like to thank S. Manabe, N.-C. Lau, K. Miyakoda, and R. S. Lindzen for helpful discussions on this topic. The figures were expertly drafted by the Scientific Illustration Group at GFDL. S. Nigam has been supported at MIT by NASA Grant NAGW-525.

REFERENCES

Bjerknes, J., 1966: A possible response of the atmospheric Hadley circulation to equatorial anomalies of ocean temperature. *Tellus,* **18,** 820–829.

——, 1969: Atmospheric teleconnections from the equatorial Pacific. *Mon. Wea. Rev.,* **97,** 163–172.

Chang, C.-P., 1977: Viscous internal gravity waves and low frequency oscillations in the tropics. *J. Atmos. Sci.,* **34,** 901–910.

Charney, J., and A. Eliassen, 1949: A numerical method for predicting the perturbations of the middle latitude westerlies. *Tellus,* **1,** 38–54.

Gill, A. E., 1980: Some simple solutions for heat-induced tropical circulations. *Quart. J. Roy. Meteor. Soc.,* **106,** 447–462.

Hayashi, Y., and D. G. Golder, 1983a: Transient planetary waves simulated by GFDL spectral general circulation models. Part I: Effects of mountains. *J. Atmos. Sci.,* **40,** 941–950.

——, and ——, 1983b: Transient planetary waves simulated by GFDL spectral general circulation models. Part II: Effects of nonlinear energy transfer. *J. Atmos. Sci.,* **40,** 951–957.

Held, I. M., 1983: Stationary and quasi-stationary eddies in the extratropical troposphere: Theory. *Large-scale Dynamical Processes in the Atmosphere,* B. J. Hoskins and R. P. Pearce, Eds., Academic Press, 127–167.

——, and B. J. Hoskins, 1985: Large-scale eddies and the general circulation of the troposphere, *Advances in Geophysics,* Vol. 28A, S. Manabe, Ed., Academic Press, 3–31.

Hendon, H. H., and D. L. Hartmann, 1982: Stationary waves on a sphere: Sensitivity to thermal feedback. *J. Atmos. Sci.,* **39,** 1906–1920.

Holton, J. R., and D. E. Colton, 1972: A diagnostic study of the vorticity balance at 200 mb in the tropics during the Northern summer. *J. Atmos. Sci.,* **29,** 1124–1128.

Horel, J. D., and J. M. Wallace, 1981: Planetary-scale atmospheric phenomena associated with the Southern Oscillation. *Mon. Wea. Rev.,* **109,** 813–829.

Hoskins, B. J., and D. J. Karoly, 1981: The steady linear response of a spherical atmosphere to thermal and orographic forcing. *J. Atmos. Sci.,* **38,** 1179–1196.

Jacqmin, D., and R. S. Lindzen, 1985: The causation and sensitivity of the Northern winter planetary waves. *J. Atmos. Sci.,* **42,** 724–745.

Lau, N.-C., 1979: The observed structure of tropospheric stationary waves and the local balances of vorticity and heat. *J. Atmos. Sci.,* **36,** 996–1016.

——, 1981: A diagnostic study of recurrent meteorological anomalies appearing in a 15-year simulation with a GFDL general circulation model. *Mon. Wea. Rev.,* **109,** 2287–2311.

——, and E. O. Holopainen, 1984: Transient eddy forcing of the time-mean flow as identified by geopotential tendencies. *J. Atmos. Sci.,* **41,** 313–328.

Lin, B.-D., 1982: The behavior of winter stationary planetary waves forced by topography and diabatic heating. *J. Atmos. Sci.,* **39,** 1206–1226.

Lindzen, R. S., T. Aso and D. Jacqmin, 1982: Linearized calculation of stationary waves in the atmosphere. *J. Meteor. Soc. Japan,* **60,** 66–77.

Manabe, S., and D. G. Hahn, 1981: Simulation of atmospheric variability. *Mon. Wea. Rev.,* **109,** 2260–2286.

Nigam, S., 1987: A steady linear primitive equation model that includes the effects of the mean meridional circulation (in preparation).

Opsteegh, J. D., and A. D. Vernakar, 1982: A simulation of the January standing wave pattern including the effects of transient eddies. *J. Atmos. Sci.,* **39,** 734–744.

Randel, W. J., and J. L. Stanford, 1985: The observed life-cycle of a baroclinic instability. *J. Atmos. Sci.*, **42,** 1364–1373.

Rowntree, P. R., 1972: The influence of tropical East Pacific ocean temperatures on the atmosphere. *Quart. J. Roy. Meteor. Soc.*, **98,** 290–321.

Sardeshmukh, P. D., and I. M. Held, 1984: The vorticity balance in the tropical upper troposphere of a general circulation model. *J. Atmos. Sci.*, **41,** 768–778.

——, and B. J. Hoskins, 1985: Vorticity balances in the tropics during the 1982–1983 El-Niño Southern Oscillation event. *Quart. J. Roy. Meteor. Soc.*, **111,** 261–278.

Schubert, S. D., and G. F. Herman, 1981: Heat balance statistics derived from four-dimensional assimilations with a global circulation model. *J. Atmos. Sci.*, **38,** 1891–1905.

Simmons, A. J., 1982: The forcing of stationary wave motions by tropical diabatic heating. *Quart. J. Roy. Meteor. Soc.*, **108,** 503–534.

——, and B. J. Hoskins, 1978: The life cycle of some nonlinear baroclinic waves. *J. Atmos. Sci.*, **35,** 414–432.

Smagorinsky, J., 1953: The dynamical influence of large-scale heat sources and sinks on the quasi-stationary mean motions of the atmosphere. *Quart. J. Roy. Meteor. Soc.*, **79,** 342–366.

Vallis, G. K., and J. O. Roads, 1984: Large-scale stationary and turbulent flow over topography. *J. Atmos. Sci.*, **41,** 3255–3271.

Wallace, J. M., 1983: The climatological mean stationary waves: Observational evidence, *Large-scale Dynamical Processes in the Atmosphere,* B. J. Hoskins, and R. P. Pearce, Eds., Academic Press, 27–52.

Wei, M.-Y., D. R. Johnson and R. D. Townsend, 1983: Seasonal distribution of diabatic heating during the First GARP Global Experiment. *Tellus,* **35A,** 241–255.

Youngblut, C. E., and T. Sasamori, 1980: The nonlinear effects of transient and stationary eddies on the mean winter circulation. Part I: The diagnostic analysis. *J. Atmos. Sci.*, **37,** 1944–1957.